8864 *Macromolecules* **2009**, *42*, 8864–8869
DOI: 10.1021/ma9016983

Macromolecules
ARTICLE

Effect of Stereochemistry on Diffusion of Polypropylene Melts: Comparison of Simulation and Experiment

Ernst von Meerwall,*,†,‡ Numan Waheed,‡ and Wayne L. Mattice‡

†*Physics Department and* ‡*Institute of Polymer Science and Polymer Engineering, The University of Akron, Akron, Ohio 44325*

Received July 30, 2009; Revised Manuscript Received September 25, 2009

ABSTRACT: We have performed dynamic Monte Carlo (MC) simulations and pulsed-gradient diffusion (D) experiments to study the effect of stereochemical composition on diffusion in linear polypropylene (PP) melts. The coarse-grained simulations were based on the rotational isomeric state model and Lennard-Jones potentials. For the proton NMR diffusion measurements we obtained three PP specimens of differing molecular weight M and dispersity, with the probability of a meso diad $P_m = 0.02$ (syndiotactic), 0.23 (atactic), and 0.89 (nearly isotactic). The experiment supplied the conversion factor K between MC steps and real time. Both simulation and M-scaled experiment found D at high P_m several times faster than at low P_m. The constant-M simulation also showed a maximum near $P_m = 0.8$ due to quenched randomness. To permit a more precise comparison with experiment, new simulations tracked the samples' P_m, mean M, and polydispersity, but K was found to vary significantly between samples. The GPC determination of M and its distribution, based on linear polyethylene calibration, may be dependent on PP stereochemistry (via D), generating misleading results. However, dilute PP diffusion measurements in a chlorinated solvent, consistent with classical dilute diffusion theory, suggest that the observed P_m-dependence of K may instead be an intrinsic feature of this MC methodology, implying that MC cannot be relied upon to provide microstructure-independent results for self-diffusion.

Introduction

In vinyl polymer melts, stereochemistry plays an important and often overlooked role in determining properties. Atactic chains behave fundamentally differently from isotactic or syndiotactic chains of the same monomer due to the quenched randomness of stereochemical sequences.[1] Melts of atactic vinyl polymers, however, cannot be easily characterized because, even in the rare case of a monodisperse system, the random stereochemistry prevents us from describing samples with a single conformational partition function. In this respect, atactic chains are similar to random copolymers, being sequences of random diads, unlike stereochemically pure isotactic and syndiotactic chains.[2,3]

Dynamic simulation allows us to focus on a particular effect through the creation of idealized samples with controlled dispersity and stereochemistry. Although dynamical Monte Carlo yields diffusion measurements that map to real time,[4] it is challenging to create simulated samples that can be compared to experimental samples. A recent comparison of trace diffusion measurements of alkanes in polyethylene using pulsed-gradient NMR and coarse-grained dynamical Monte Carlo simulation shows excellent and consistent agreement once the relationship between Monte Carlo steps (MCS) and real time has been established.[5] These results confirm that this scaling relation between simulation and experiment is independent of the molecular weight of the polymer. Such independence, particularly at molecular weights exceeding several monomers, is expected for the detailed methodology used.

A more rigorous test for the mapping between dynamical Monte Carlo and pulsed-gradient NMR diffusion measurements is provided by stereochemical differences: it is not clear *a priori* that the same scaling factor should apply for moves conducted on different stereochemical centers. In addition, comparison with experimental samples can yield the relative importance of controlling dispersity and tacticity. Recent simulations, which assumed the scaling factor to be the same, have shown an enhanced diffusion effect for atactic polypropylene (PP) chains.[6] Since this result had not been observed experimentally due to the unavailability of appropriate samples, the operational details of the simulation method must be carefully examined. We therefore wish to test the hypothesis that the scaling factor between Monte Carlo steps and real time is not stereochemically dependent. The assumptions implicit in the stylized representation of the molecules and their dynamics in this and other MC methods are too complex to permit full confidence in the consistency of the dynamical predictions; at the current state of knowledge the comparison between simulation and experiment is best regarded as an empirical issue. However, this comparison is complicated experimentally by the limited ability to create and accurately characterize monodisperse systems of known tacticity and theoretically by the difficulty in simulating long PP chains.

An opportunity presented itself to substantiate dynamical Monte Carlo simulation of diffusion in stereochemically varied melts by conducting pulsed-gradient ^{1}H NMR diffusion experiments on well-characterized samples of polypropylene. Three specimens of polypropylene were uniquely synthesized by Prof. Geoffrey Coates, yielding unusually low-dispersity samples that facilitate comparison with ideal simulations.

In this report, we attempt to validate the use of a single scaling factor between Monte Carlo steps and real time for three experimental samples of PP with differing tacticity, created to best deal with the issues of molecular weight and polydispersity. We perform pulsed-gradient NMR diffusion measurements on

*To whom correspondence should be addressed: e-mail evonmee@uakron.edu; Tel (330) 972-5376; Fax (330) 972-5396.

 Published on Web 10/02/2009 © 2009 American Chemical Society

the three samples of PP and corresponding monodisperse simulations of the same molecular weight and probability of meso diad (P_m). We determine the values for the scaling factor and propose explanations for these results. Further simulation is conducted to determine whether polydispersity of the experimental samples needs to be taken into account.

Methods

Polypropylene Samples. Samples and their characterization were obtained from Dr. G. Coates. Details of the samples are given in Table 1. Molecular weight M_n and polydispersity M_w/M_n were determined by gel permeation chromatography at 140 °C in 1,2,4-trichlorobenzene relative to polyethylene standards. The probability of meso diad P_m was determined using ^{13}C NMR spectroscopy.

Samples for the melt diffusion measurements were prepared by inserting 200−300 mg of polypropylene solids into 7 mm o.d. NMR sample tubes. Samples were compacted mechanically, after which the tubes were filled with nitrogen and flame-sealed. To obtain a clean meniscus in the melted state and eliminate bubbles, the samples were heated overnight to 150 °C. During measurement, the samples were heated to 180 °C for 45 min. No evidence of thermal degradation was found.

Pulsed-Gradient ^1H NMR. Diffusion coefficients were measured using proton pulsed-gradient spin-echo NMR (PGSE NMR). This technique is based on pulsed nuclear magnetic resonance; the details of our implementation of PGSE NMR have been described previously.[7] To summarize, the 33 MHz Spin-Lock CPS-2 spectrometer was employed to produce a stimulated echo following the last 90° pulse in a three-pulse radio-frequency sequence. The sequence was coordinated with a matched pair of pulsed magnetic field gradients of magnitude $G = 215$ G/cm, separated by $\Delta = 150$ ms. A steady gradient of magnitude $G_0 = 0.3$ G/cm was also applied for experimental convenience by narrowing the echo signal. As a result of the gradient pulses, the spin-echo height A in the sample is attenuated as the sample molecules diffuse. The gradient pulse duration δ was adjusted in 15−20 steps until the echo signal was reduced to the background noise level. Audio signals were obtained using single sideband radio-frequency phase-sensitive detection offset by 3 kHz from the reference frequency, followed by Hamming-windowed magnitude Fourier transforms integrated over the echo peak, corrected for magnitude baseline noise. Echo height measurements were averaged over 6−12 signal passes. Results were then analyzed off-line using the latest version of the Fortran code DIFUS5.[8] The echo attenuation is expected to follow the general form

$$\frac{A(X)}{A(0)} = \sum_i w_i \exp[-\gamma^2 D_i X] \qquad (1)$$

with $\sum_i w_i = 1$, where γ is the proton gyromagnetic ratio and $X = \delta^2 G^2(\Delta - \delta/3)$ + small correction terms in GG_0.

The echo attenuation data were analyzed according to several models, of which two were selected as most appropriate. The first of these is a mapping of component D_i to melt mass fraction M_i based on the measured polydispersity using either Rouse or reptational scaling as appropriate given literature estimates[9] for the entanglement onset molecular weight M_e.[10] The second is a generalized log−normal diffusivity distribution model in which both the mean diffusion rate and the rate distribution are adjustable in a fit to the data; here the source of the diffusivity distribution remains unspecified. In both models, nine discrete amplitude-weighted components i are used to approximate the continuum. The dispersity-based model, preferable in principle, adequately described all three sets of our data provided that full reptational scaling $D \approx M^{-2}$ was assumed. All three fits are rendered somewhat inferior if Rouse scaling $D \approx M^{-1}$ within the ensemble is substituted; the difference is greatest in the case of iPP, which has the highest polydispersity and is thus the most sensitive to scaling. Lacking guidance due to the relative scarcity of reliable data on M_e for the PP melt system as a function of tacticity,[9] it is tentatively concluded that in each case the ratio M_n/M_e is likely to exceed unity, i.e., that all three specimens are at least marginally entangled. Nevertheless, for the final analysis of our data the average diffusion coefficients reported here are those obtained using the generalized log−normal distribution model, which in each case provides additional improvements in the goodness of fit (chi-square per degree of freedom). Figure 1 shows the echo attenuations and log−normal model fits for our three specimens.

Table 1. Characteristics of Polypropylene Samples

sample	amount (g)	M_n (g/mol)[a]	M_w/M_n[a]	P_m[b]	T_g (°C)[c]	T_m (°C)[c,d]
sPP	0.94	12300	1.05	0.02	−3.4	140.3
aPP	0.43	5300	1.03	0.23	−9.7	n.d.
iPP	0.65	9900	1.24	0.89	−13.1	108.7

[a] Molecular weight and molecular weight distribution were determined by gel permeation chromatography at 140 °C in 1,2,4-trichlorobenzene relative to polyethylene standards. [b] Probability of meso diad was determined using ^{13}C NMR spectroscopy. [c] Glass transition and melting temperatures were determined from differential scanning calorimetry (second heating run). [d] For the melting temperature, atactic PP melting temperature could not be detected; for sPP the value is the average of two adjacent melting transitions.

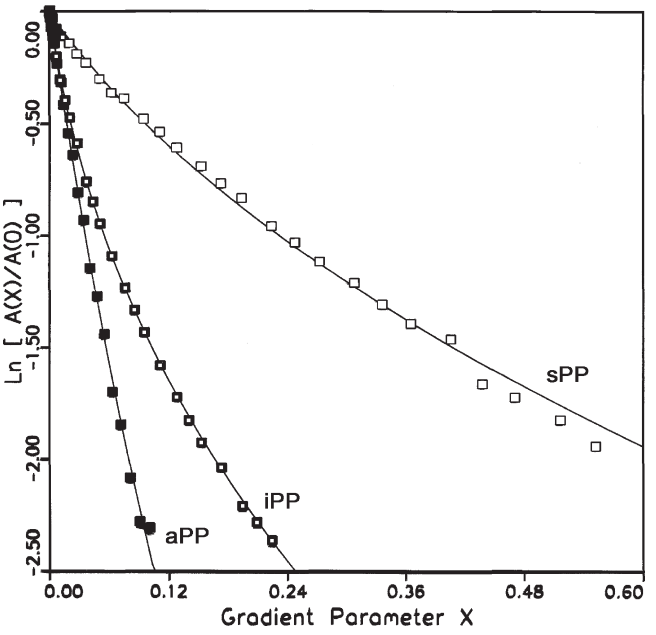

Figure 1. Diffusional echo attenuations in the three polypropylene melt specimens (symbols) together with fitted models (lines) postulating log−normal distributions of diffusion rates of optimized means and standard deviations (see Table 3).

Dilute Diffusion Measurements. To test for the possibility that the GPC determination of the samples' molecular weight may suffer a systematic misleading dependence on microstructure as a result of differences in (dilute) diffusion rates, proton diffusion measurements were conducted on each specimen dissolved in a common solvent trichloroethylene at 70 °C, at two concentrations below 2 wt %. The results were extrapolated to zero PP concentration to obtain the infinite-dilution values. Careful corrections for the presence and diffusion of trace protonated species in the chlorinated solvent were required. The interpretive model successfully fitted was based on the samples' polydispersity as described above for the melts, but using Rouse rather than reptational ensemble M-scaling.

Coarse-Grained Monte Carlo. Dynamical Monte Carlo simulations of diffusion in the polypropylene melt system at fixed

Table 2. Details of Monodisperse Polypropylene Simulations

sample	M_n (g/mol)	M_w (g/mol)	P_m	beads per chain	parent chains	lattice size	replicas
sPP	12300	12300	0.02	293	40	46	3
aPP	5300	5300	0.23	126	21	28	3
iPP	9900	9900	0.89	236	28	38	3

molecular weight M_n as a function of the probability of meso diads (P_m) have been comprehensively described in a previous publication.[6] Briefly, the coarse-grained model[11] is based on a high-coordination (second-nearest-neighbor diamond) lattice, with each C_3H_6 monomer (42 g/mol) represented as a bead placed at the stereochemical center; any snapshot in the simulation can be easily reversed to the atomistic detailed chain. Short-range interactions between bonded beads are based on the rotational isomeric state model[12] according to the stereochemistry of a particular dyad as previously parametrized for polypropylene.[3] Long-range interactions between nonbonded beads are represented by discretized 6−12 Lennard-Jones potentials extending to either two or three neighbor shells.[13] Bond lengths and bulk densities correspond to actual values. The initial simulations[6] build 64 PP chains of 25 bonded beads on a 24 × 24 × 24 unit cell, with a lattice spacing of 2.5 Å. Experimental temperature is correctly incorporated in the Metropolis algorithm for kinetics and dynamics; the ensemble is maintained under NVT conditions. Single bead and 2−6 bead pivot rotation moves are used; the former, permitting occasional chain crossings, serves for equilibration purposes only. In the present work, a first attempt was made to correlate the results of these small-box simulations with those of the experimental measurements, by employing an M-scaling based on polyethylene, with indifferent results (see below).

Therefore, new dynamical Monte Carlo simulations were conducted to duplicate the attributes of the three samples, i.e., maintaining the samples' M_n as well as P_m. The new simulations were conducted at 180 °C; the number of parent chains and the lattice size were chosen to maintain a melt density of 0.76 g/cm^3 and structured such that each cell dimension (lattice size) is twice the average radius of gyration of the chains. Three independent replicas were simulated at each P_m. Details are given in Table 2.

Systems were equilibrated for 4 million MCS. The dynamics were then simulated using the two-bead moves for 10 million MCS. Dynamical data were used to calculate the mean-squared displacements of the centers-of-mass of each chain over different time intervals. Data over time intervals of 2−8 million MCS were used to calculate diffusion coefficients, to ensure that measurements are not influenced by non-Fickian behavior over short intervals or statistical error due to the small number of measurements over long intervals.

Results and Discussion

Experiments in the Melts. The diffusion coefficients extracted from the echo attenuation data in our three samples, for the two relevant models, are shown in Table 3. It should be noted that separate spin−spin relaxation experiments yielded nearly single-exponential relaxation decays with T_2 near 50 ms without appreciable differences among the samples.

While we tentatively accept the measured M_n for analyzing the diffusion results, we note that the GPC technique used to measure molecular weight leaves several unanswered questions that will be discussed later.

Fixed-*M* Simulations. A comparison between the experimental data and the original small-box simulations (see ref 6) depended on two scalings. First, the molecular weight of this simulation, 25 monomers (M = 1050), was rather smaller than those of any of the samples. Thus, the experimental D values were scaled up in rate in accordance with $D \sim M^{-1.85}$, the exponent taken from the D (M)-dependence in the n-alkane/polyethylene system at this temperature.[14,15] This

Table 3. Diffusion Coefficients from PGSE-NMR Measurements Using Two Models

sample	M_n	M_w/M_n	P_m	model[a]	D_{Mn} or $\langle D \rangle$	reduced σ	chi-square-Nu
sPP	12300	1.05	0.03	A	5.61×10^{-09}		3.84
				B	6.19×10^{-09}	1.37	2.64
aPP	5300	1.03	0.23	A	3.85×10^{-08}		1.00
				B	3.94×10^{-08}	0.62	0.78
iPP	9900	1.24	0.89	A	2.63×10^{-08}		1.06
				B	2.70×10^{-08}	1.85	0.43

[a] Model A is based on measured GPC polydispersity and assumes reptational ensemble scaling $D \approx M^{-2}$. Model B represents a log−normal D-distribution with geometric mean $\langle D \rangle$ and reduced standard deviation σ. All D are given in cm^2/s.

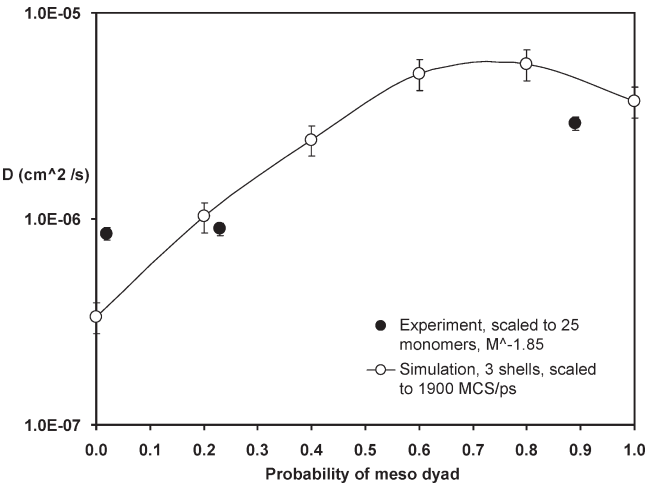

Figure 2. Comparison of small-box monodisperse simulation results (ref 6) with experimental diffusion measurements scaled to a common M = 1050 using a scaling law derived from the alkane/polyethylene system (see text) and compromising on a conversion factor of 1900 MCS/ps.

extrapolation is too distant to inspire confidence, and the approximation of PP to PE itself is regarded as highly tentative. The second scaling, endemic to dynamic Monte Carlo, involves deriving a conversion of MC steps to real time. Shown in Figure 2 is the result, with a best compromise conversion factor of 1900 MC steps per picosecond.

While the overall increase of D with P_m is captured in general terms, the comparison falls substantially outside the combined uncertainties of simulation and experiment. This state of affairs was the motivation to perform further simulations designed to achieve equivalence with the experimental specimens.

Experiment-Tracking Simulations. The results of the new simulations, based on the samples' measured M_n and P_m, but without taking into account polydispersities or their differences among the samples, are given in Table 4. Diffusion coefficients reported are center-of-mass values.

Because of the relatively large polydispersity of the iPP sample, an additional simulation was conducted to better reproduce the properties of this experimental sample, by correctly modeling both M_n and M_w. While there are several bidisperse systems that will correctly generate these values, we chose the values for the length of each chain and the

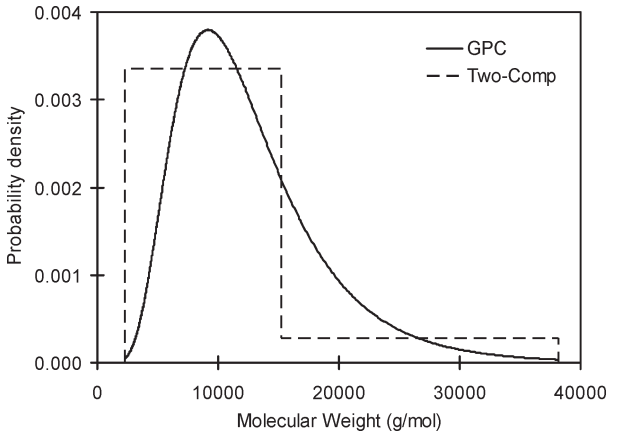

Figure 3. Molecular weight distribution from GPC measurements (curve) and as coarsely rendered by a corresponding bidisperse model.

Table 4. Properties of Monodisperse Simulation Systems

sample	P_m	M_n	parent chains	ind sim	diffusion (cm^2/million MCS)
sPP	0.02	12300	40	3	1.9×10^{-18}
aPP	0.23	5300	21	3	1.2×10^{-17}
iPP	0.89	9900	28	3	1.7×10^{-17}

Table 5. Molecular Weight Properties of iPP Experimental Sample and Simulations

sample	M_n (g/mol)	M_w (g/mol)
experimental	9900	12200
monodisperse simulation	9900	9900
bidisperse simulation	9900	12200

number of each component to best match the approximately log−normal distribution as measured. Figure 3 shows this GPC M-distribution. For our bidisperse approach, this distribution is divided into two parts to create a histogram, with the cumulative probability of each part yielding the fraction of the component. The molecular weights of each component are chosen to minimize the error in M_n and M_w, yielding the histogram shown in Figure 3.

The simulation consists of six chains of 533 beads (22 000 g/mol) and 40 chains of 193 beads (8100 g/mol), on a $45 \times 45 \times 45$ lattice. Table 5 summaries the properties of the experimental sample, the original monodisperse simulation, and the bidisperse simulation.

The inclusion of bidispersity results in an average center-of-mass diffusion coefficient for each of the two iPP components. These are shown in Table 6 together with the resulting number-average diffusion coefficient $D(M_n)$ characterizing the mixture.

It is of interest to note that the ratio of the two component D values compared with the corresponding ratio of M generating them corresponds to a scaling M exponent of −1.4. Thus, the simulation is still in the midst of the transition between Rouse-like and entangled diffusion, whereas the experiment already appears to be consistent with entangled diffusion. The simulation's mean diffusion coefficient $D(M_n)$ for the bidisperse system is 3.8×10^{-17} cm^2/million MCS, which is somewhat higher than that of the monodisperse system. The large number of short chains required to duplicate the number-average and weight-averaged molecular weights skew to a faster average diffusion for the overall mixture.

Average diffusion coefficients in cm^2/s measured by PGSE NMR are shown in Table 7. Also shown are the diffusion coefficients for the simulations in cm^2 per million MCS and

Table 6. Diffusion of Components in Bidisperse Mixture

component	M (g/mol)	mass fraction	diffusion (cm^2/million MCS)
short	8100	0.71	4.9×10^{-17}
long	22000	0.29	1.2×10^{-17}
weighted mean		1.00	3.8×10^{-17}

Table 7. Diffusion Coefficients for Experiment and Simulation

sample	exptl D (cm^2/s)	simul D ($cm^2/10^6$ MCS)	ratio of MCS/ps
sPP	6.20×10^{-9}	1.9×10^{-18}	3260
aPP	3.95×10^{-8}	1.2×10^{-17}	3290
iPP	2.70×10^{-8}	1.7×10^{-17}	1590

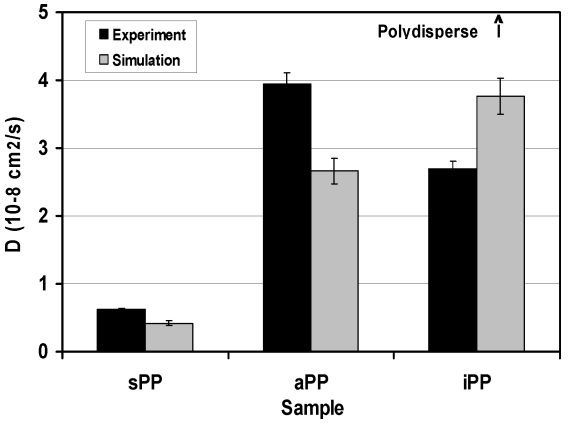

Figure 4. Diffusion coefficients in three PP specimens from experiments and simulations. Simulation results are scaled using the single best-fit conversion factor (monodisperse) of 2220 MCS/ps.

the value of the ratio of MCS to real time calculated individually to match each of the three samples. A significant difference is seen between the ratio required to duplicate diffusion rates in iPP vs in sPP and aPP. Attempts to model all three systems using the same ratio were conducted by minimizing the cumulative error of all three samples, leading to a ratio of 2220 MCS/ps. This approach does not yield fully convincing results, as shown in Figure 4.

The ratio of 2220 MCS/ps is fitted by minimizing the error of all three measurements simultaneously, but the fit results in deviations from the experimental values somewhat outside combined uncertainties. Still, the improvement of the agreement by comparison between the original small-M simulations and the scaled experiment is reassuring.

Discussion. We note that the diffusion rates are a function of both the molecular weight and the stereochemistry, making their absolute value difficult to interpret. In the case of the simulations, the relative magnitude of the diffusion rates follows the relative magnitude of the molecular weights, indicating that molecular weight effect dominates the stereochemical effect in the simulation. Stereochemistry plays a role as well, but it is more difficult to isolate, given the large range of molecular weights in the samples.

The ratios of MCS to real time are quite similar between the sPP and aPP sample, but the iPP sample shows a significant difference. While the probability of meso diad is similar in the sPP and aPP case compared to iPP, the more obvious difference is that of the polydispersity (see Table 1), which may mask the effects of stereochemistry. The difference in the ratio for iPP compared to aPP and sPP may be due to the fact that, in the case of iPP, a polydisperse sample is being compared to a monodisperse (or bidisperse) simulation. This is of great interest considering that a polydispersity

ratio of 1.24 for iPP is regarded as extremely well controlled for most commercial PP samples. Further analysis of the molecular weight distribution and its effect on diffusion is needed to determine whether and to what extent stereochemistry affects the scaling factor between simulation and experiment.

The comparison of the iPP experimental sample to the bidisperse system reveals that adding a second component to better match the experimental molecular weight distributions leads to an experiment-to-simulation scaling of 710 MCS/ps. This is much less than that predicted in the monodisperse system, leading to two conclusions. First, the addition of polydispersity cannot account for the difference in scaling factors between the isotactic and syndiotactic systems, since addition of polydispersity takes the scaling further away from the observed scaling of ~3275 ± 50 MCS/ps for the other two systems. Second, possession of correct data for the molecular weight distribution is vital since results depend so strongly on the details of the distribution.

The characterization of the molecular weight distribution for vinyl polymers requires a further note. The measurement of molecular weight and polydispersity of the samples may in fact account for the difference in the scaling for samples with different tacticity. Given the fact that the calibration standard for the GPC molecular weight measurement is polyethylene, one should question whether the technique is capable of giving accurate measurements for stereochemically varied chains. In fact, since GPC operates on the basis of hydrodynamic volume, it is more likely that diffusion itself is implicit in the molecular weight determination. Therefore, isotactic and syndiotactic samples of polypropylene with identical actual molecular weights may display different apparent molecular weights when using GPC, since they have different diffusion rates and hydrodynamic volumes due to stereochemistry. Unfortunately, attempts to use other techniques for measuring molecular weight distribution were unsuccessful. Because the molecular weights were too high, attempts at mass spectrometry techniques by Dr. David Dabney and Professor Wesdemiotis at the University of Akron were unable to yield reliable data. For this reason, the GPC data were taken at face value for this analysis.

Older work by this laboratory,[16] in a set of 14 plasticizer species intended for use with poly(vinyl chloride) (PVC), had clearly demonstrated that although their diffusion rates in their own melts, as well as dissolved in PVC, were strongly dependent on molecular shape as well as molecular weight, their diffusion rates extrapolated to infinite dilution, D_0, in a good small-molecule solvent lacked any shape dependence, resembling the classical dilute-solution power-law variation with molecular weight alone. These observations provided an incentive to conduct similar measurements for our PP samples. The results are shown in Figure 5.

Although the M and D_0 ranges are comparatively small, substantial P_m-dependent deviations of M(GPC) from some putatively correct value should be detectable. The minimum required to remove the apparent discrepancy for the iPP sample in the scaling factor of MCS to real time, a horizontal relative shift of M by a factor approaching two, would be clearly seen as anomalous. A comparison of the M-dependence of D_0 with a power-law slope near −0.5 to −0.6 based on classical dilute-solution theory shows no substantial departures outside experimental uncertainty. In the absence of such a deviation, the case for a P_m-dependent GPC error cannot be supported, leading to the tentative conclusion that some, or much, of the P_m-dependence of the scaling may be an intrinsic feature of our MC methodology. In that case, the quantitative interpretation of the trend seen in the simulations in Figure 2, taken from ref 6, would also require appropriate adjustment, although the qualitative conclusions remain unaltered.

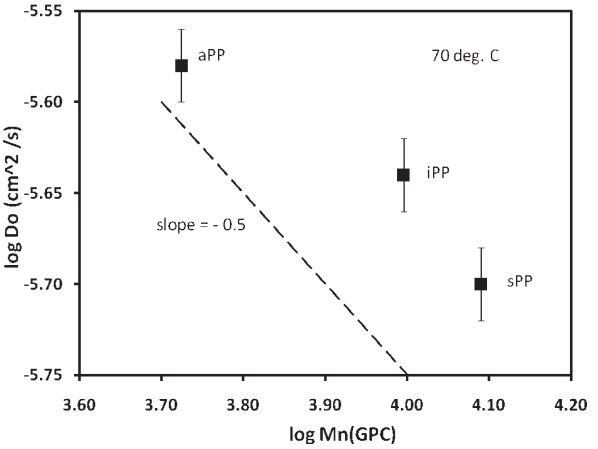

Figure 5. Diffusion coefficients of the three PP specimens dissolved in trichloroethylene, extrapolated to infinite dilution, as a function of the GPC-determined molecular weight. The dashed line suggests the Flory M-dependence (arbitrary intercept) of D_0 in beta solvents.

It appears evident that the operation of dynamic MC is less straightforward than our earlier results under less arduous conditions had optimistically led us to expect. Although the evidence presented here is necessarily somewhat indirect, we suggest that variations in molecular architecture and microstructure most likely do significantly affect the success of simulated diffusional steps and hence the scaling with real time. This inference might well be of interest to other workers using MC methodology to simulate dynamics in assemblies of large molecules. The additional effects of polydispersity represent a complicating factor which deserves further exploration.

Conclusions

We have conducted dynamical Monte Carlo simulations and pulsed-gradient spin-echo NMR experiments on polypropylenes with different tacticity. Isotactic, atactic, and syndiotactic polypropylene samples with unusually low polydispersity were analyzed to yield diffusion coefficients. Analogous simulations were conducted on monodisperse systems of the same average molecular weight and probability of the meso diad. While the scaling of Monte Carlo steps to picoseconds was consistently ~3200 MCS/ps for the syndiotactic and atactic samples, the isotactic sample resulted in a scaling of ~1600 MCS/ps. We note that the isotactic sample differs from the syndiotactic and atactic sample both in the probability of meso diad (the atactic sample is much closer to syndiotactic PP) and in the polydispersity. An additional simulation of a bidisperse iPP system was conducted to match both the number-averaged and mass-averaged molecular weights. However, this refinement of the molecular weight distribution generated a scaling even further from the syndiotactic and atactic systems than the monodisperse iPP simulation. We suggest that the GPC measurement technique should be called into question for vinyl polymers. This technique implicitly assumes that stereochemistry is not affecting the elution time of the sample, even though we have previously established that stereochemistry strongly affects diffusion in the melts. However, our dilute diffusion measurements, a better basis for comparison because of their closer resemblance to GPC practice, offer no direct support for this hypothesis. Thus, we are unable to verify that microstructure does not affect the scaling between Monte

Carlo steps and real time in the present MC methodology. It is known[17] that relatively subtle changes in microstructure can have major effects on the physical properties of polymer melts and blends; the current findings likely reflect the difficulty of reproducing such effects in simulations. This work, thus, represents a note of caution to users of MC simulations to avoid their uncritical use under changing conditions of molecular architecture, microstructure, and polydispersity.

Acknowledgment. The authors thank J. Rose, J. Edson, and Professor G. Coates of Cornell University for the samples and their characterization. We are grateful to D. Dabney and Professor. C. Wesdemiotis at The University of Akron for discussions on molecular weight characterization and for their attempts to use mass spectrometry to determine molecular weights for our specimens. This research was supported by the National Science Foundation under Grant DMR 04 55117.

References and Notes

(1) Mattice, W. L.; Waheed, N. *Macromolecules* **2006**, *39*, 2380–7.
(2) Flory, P. J. *Statistical Mechanics of Chain Molecules*; Wiley: New York, 1969.
(3) Suter, U. W.; Pucci, S.; Pino, P. *J. Am. Chem. Soc.* **1975**, *97*, 1018–23.
(4) Fichthorn, K. A.; Weinberg, W. H. *J. Chem. Phys.* **1991**, *95*, 1090–6.
(5) von Meerwall, E. D.; Lin, H.; Mattice, W. L. *Macromolecules* **2007**, *40*, 2002–7.
(6) Waheed, N.; Mattice, W. L.; von Meerwall, E. D. *Macromolecules* **2007**, *40*, 1504–11.
(7) Iannacchione, G.; von Meerwall, E. *J. Polym. Sci., Part B: Polym. Phys.* **1991**, *29*, 659–68.
(8) von Meerwall, E. D.; Ferguson, R. D. *Comput. Phys. Commun.* **1981**, *21*, 421–9.
(9) Fetters, L. J.; Lohse, D. J.; Colby, R. H. In *Physical Properties of Polymers*; Mark, J. E., Ed.; American Institute of Physics: Woodbury, NY, 1996; Chapter 24.
(10) von Meerwall, E.; Palunas, P. *J. Polym. Sci., Polym. Phys. Ed.* **1987**, *25*, 1439–1457.
(11) Lin, H.; Mattice, W. L.; von Meerwall, E. D. *J. Polym. Sci., Part B: Polym. Phys.* **2006**, *44*, 2566–71.
(12) Mattice, W. L.; Suter, U. W. *Conformational Properties of Large Molecules. The Rotational Isomeric State Model in Macromolecular Systems*; Wiley: New York, 1994.
(13) Clancy, T. C.; Mattice, W. L. *J. Chem. Phys.* **2000**, *112*, 10049–55.
(14) von Meerwall, E.; Beckman, S.; Jang, J.; Mattice, W. L. *J. Chem. Phys.* **1998**, *108*, 4299–4304.
(15) von Meerwall, E.; Feick, E.; Ozisik, R.; Mattice, M. L. *J. Chem. Phys.* **1999**, *111*, 750–757.
(16) von Meerwall, E.; Skowronski, D.; Hariharan, A. *Macromolecules* **1991**, *24*, 2441–2449.
(17) see, for example Mattice, W. L.; Helfer, C. A.; Rane, S. S.; von Meerwall, E. D.; Farmer, B. L. *J. Polym. Sci., Part B: Polym. Phys.* **2005**, *43*, 1271–1282.